Research on the Influence of Stress Relaxation on the Sealing Performance of the Packer Under HTHP

Gang Hu · Yepeng Liu · Guorong Wang · Wei Wu ·
Zhaoqiang Xu · Kunrong Shen

Abstract   As a key tool in hydraulic fracturing, the packer plays a vital role in the process of unconventional oil and gas production. Its sealing performance has a significant impact on production. The packer is in high-temperature and high-pressure (HTHP) environment for a long time. It is easy to produce significant stress relaxation, which affects the sealing performance of the packer. In this paper, rubber foundation tests at 150 °C temperature were carried out. The hyperelastic–viscoelastic model of the rubber material was determined. The influence of the stress relaxation on its sealing performance was investigated. In addition, the effects of setting load, height, inner diameter, and outer diameter on the sealing performance were systematically investigated. The findings show that under HTHP, the stress relaxation phenomenon leads to a 6.9% decrease in peak shear stress, 10.3% decrease in peak von Mises stress, and 6.7% decrease in peak contact stress, reducing the risk of damage to the packing element and leading to a decrease in its sealing performance. In addition, it was found that increasing the setting load can significantly increase the contact stress, which also increases the risk of damage. When increasing the height, the peak shear stress and peak contact stress do not change much but can significantly reduce the peak von Mises stress. When increasing the inner diameter, the peak shear stress and peak contact stress show a trend of first increasing and then decreasing, and the peak von Mises stress has been decreasing. Increasing the outer diameter can better improve the force situation, increase the contact stress, and make the contact stress distribution more uniform. It is necessary to consider the influence of stress relaxation on the sealing performance of the packer under HTHP; meanwhile, this paper has guiding significance for the design of packer structures.

Keywords   Packer · Viscoelasticity · Stress relaxation · Hyperelastic–viscoelastic model · Sealing performance

G. Hu (✉) · Y. Liu · G. Wang · W. Wu · Z. Xu
School of Mechatronic Engineering, Southwest Petroleum University, Chengdu 610500, China
e-mail: swpu_hugang@163.com

G. Hu · Y. Liu · G. Wang · Z. Xu
Energy Equipment Research Institute, Southwest Petroleum University, Chengdu 610500, China

K. Shen
School of Engineering, Southwest Petroleum University, Nanchong 637001, China
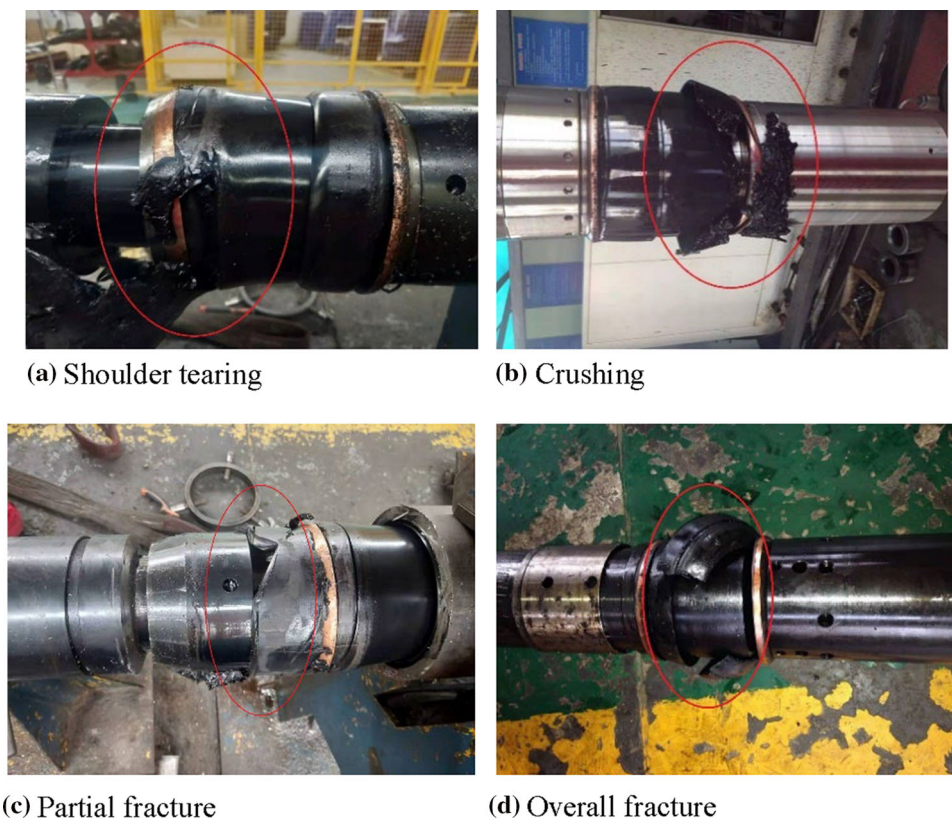
Introduction

In the middle of the twentieth century, hydraulic fracturing was proposed to increase the permeability of the reservoir. In the process of hydraulic fracturing, the harsh conditions of HTHP at the bottom of the well put higher requirements on the packing element. Its working performance directly affects the production cost and the economic efficiency of the enterprise [1]. As the sealing core component of the packer, the packing element, when working under HTHP, is prone to shoulder protrusion, stress relaxation, aging [2–6], and other phenomena, resulting in shoulder tearing, crushing, partial fracture, or even overall fracture of the packing element, which eventually leads to seal failure of the packer, as shown in Fig. 1.

In recent years, research on HTHP packer has attracted increasing attention. Guo et al. optimized the wall thickness parameters of the packing element by nonlinear FEA

842

J Fail. Anal. and Preven. (2022) 22:841–857

Fig. 1 Packing element failure


(a) Shoulder tearing

(b) Crushing

(c) Partial fracture

(d) Overall fracture

to improve its pressure-bearing capacity [7]. James and others have studied to increase the temperature and pressure resistance of permanent packers from 69 MPa and 121 °C to 138 MPa and 132 °C [8]. Hua et al. analyzed the causes of completion packer failure and proposed some preventive measures [4]. Zheng et al. developed TPV-based swellable polymers for use in high-temperature packing element materials based on experiments, which resulted in higher strength and heat resistance of the packing element [9]. Lan et al. combined simulations and experiments to study the sealing performance of the packing element at HTHP and concluded that the combination of a single packing element with an expanding support ring and AFLAS material is more conducive to sealing [10]. Duan et al. proposed a formulation of a HTHP packing element material, which was able to successfully pass the 200 °C, 70 MPa oil seal 30 min without pressure drop or leakage test [11]. Dong et al. designed an anti-shoulder protrusion structure packer for the shoulder protrusion phenomenon of the packing element during fracturing [12]. Han et al. investigated the mechanical behavior of packer cavities at HTHP based on FEA and experiments, and optimized the structural parameters [13]. Zheng et al. optimized the structural parameters of the sealer rubber cylinder by nonlinear FEA, which provided guidance for its design [14].

As can be seen, researchers have conducted a lot of research on HTHP packers in terms of material properties and structural parameters. However, in the process of hydraulic fracturing, the rubber material will experience significant stress relaxation because the packer needs to work in HTHP environment for a long time. Stress relaxation is the continuous decay of stress with time in a constant state of deformation [15]. It affects not only the load-bearing capacity of rubber seals, but also their sealing performance. Therefore, it reduces the safety of rubber seals in practice, reduces the service life of rubber seals, and makes it difficult to ensure the working requirements of long-term sealing [16].

Currently, there is a large amount of research on the stress relaxation phenomenon in rubber. Through experiment analysis, it was found that the increase in temperature accelerates the stress relaxation process in hydrogenated nitrile rubber (HNBR) [17]. Wang et al. used FEA to obtain the variation law of the contact stress between sphere-tapered surface considering stress relaxation [18]. Wang and Zhang successively analyzed the stress relaxation of O-rings under different parameters based on the rubber hyperelastic–viscoelastic model and found that the increase in temperature causes a significant increase in the stress relaxation rate and reduces the reliability of the seal [19, 20].

Fig. 2 Uniaxial tension experiments process

(a) Specimen size   **(b)** Specimen   **(c)** Uniaxial tensile experiment
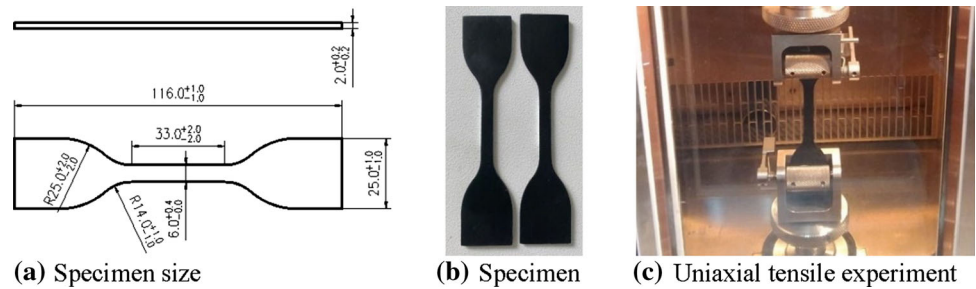
In summary, many scholars have conducted researchs on HTHP packer and rubber stress relaxation phenomenon, but there are few research studies on the effect of stress relaxation on seal performance of packers under HTHP. This paper takes Y445-115 packer as an example, and analyzes the influence of stress relaxation on the performance of the packer. Meanwhile, based on considering rubber stress relaxation, the influence of setting load and packing element structure parameters on the performance of the packer is explored. Firstly, uniaxial tensile, uniaxial compression and stress relaxation tests at high temperatures were carried out. Secondly, hyperelastic-viscoelastic model parameters were obtained based on the test data, and their correctness was verified. Furthermore, laboratory bench experiments are carried out to verify the correctness of the FEA method. Finally, a 2D axisymmetric FEA model was developed to investigate the effect of stress relaxation and key structural parameters on the sealing performance of the packing element.

Packing Element Constitutive Model

Constitutive Model Theory

The packing element is the core element of the packer to achieve a seal, and its mechanical properties are very sensitive to temperature, loading rate, and strain rate. It is hyperelastic and viscoelastic. The strain energy density function is used to characterize the mechanical properties of a hyperelastic material. The strain energy function is expressed as

$$W = W(I_1, I_2, I_3) \qquad \text{(Eq 1)}$$

where λ_1, λ_2, and λ_3 are the three invariants of the Green strain tensor:

$$I_1 = \lambda_1^2 + \lambda_2^2 + \lambda_3^2 \qquad \text{(Eq 2)}$$

$$I_2 = \lambda_1^2\lambda_2^2 + \lambda_2^2\lambda_3^2 + \lambda_3^2\lambda_1^2 \qquad \text{(Eq 3)}$$

$$I_3 = \lambda_1^2\lambda_2^2\lambda_3^2 \qquad \text{(Eq 4)}$$

where λ_1, λ_2, and λ_3 are the main elongations.

After preferences, the Yeoh model is used in this paper. The Yeoh model is a simplified polynomial hyperelastic model [21]. The strain energy function is expressed as

$$W = \sum_{i=1}^{N} C_{i0}(\overline{I_1} - 3)^i + \sum_{K=1}^{N} \frac{1}{d_K}(J - 1)^{2K} \qquad \text{(Eq 5)}$$

According to the simplified form commonly used in the Yeoh equation, N generally takes 3; for incompressible material, J takes 1 [22]. The strain energy is expressed as

$$W = C_{10}(I_1 - 3) + C_{20}(I_1 - 3)^2 + C_{30}(I_1 - 3)^3 \qquad \text{(Eq 6)}$$

There are several viscoelastic models, typically Maxwell fluid model, Kelvin solid model, standard linear solid model, generalized model, etc.

In this paper, the generalized Maxwell viscoelastic model is used. In FEA soft, the Prony level is used to express the time-dependent properties of the mechanical properties, and the expression for the shear relaxation modulus [23] is

$$G_R(t) = G_0\left(1 - \sum_{i=1}^{n} \overline{g}_i^p(1 - e^{-t/\overline{\tau}_i^G})\right) \qquad \text{(Eq 7)}$$

where $G_R(t)$ is the instantaneous value of shear relaxation modulus; G_0—initial value of shear relaxation modulus; $\overline{g}_i^p$—dimensionless material constant; $\overline{\tau}_i^G$—relaxation time.

The instantaneous value of the shear relaxation modulus is divided by the initial value to obtain the dimensionless shear relaxation modulus, as shown in Eq. 8:

$$g_R(t) = \frac{G_R(t)}{G_0} = 1 - \sum_{i=1}^{n} \overline{g}_i^p(1 - e^{-t/\overline{\tau}_i^p}) \qquad \text{(Eq 8)}$$

where $G_0 = G_R(0)$, $g_R(0) = 1$, and $g_R(\infty) = G_\infty/G_0$.

Material Experiment

To determine the parameters of the hyperelastic-viscoelastic constitutive model of rubber at 150 °C, experiments were carried out using an Instron electronic universal testing machine. According to ISO 37:2011, ISO 3384:2005, and ISO 7743:1989, uniaxial tensile tests, uniaxial compression tests, and compressive stress relaxation tests were performed on HNBR. Rubber material hardness is 80SHA.

Fig. 3 Uniaxial compression experiments process

(a) Specimen size

(b) Specimen

(c) Uniaxial compression experiment
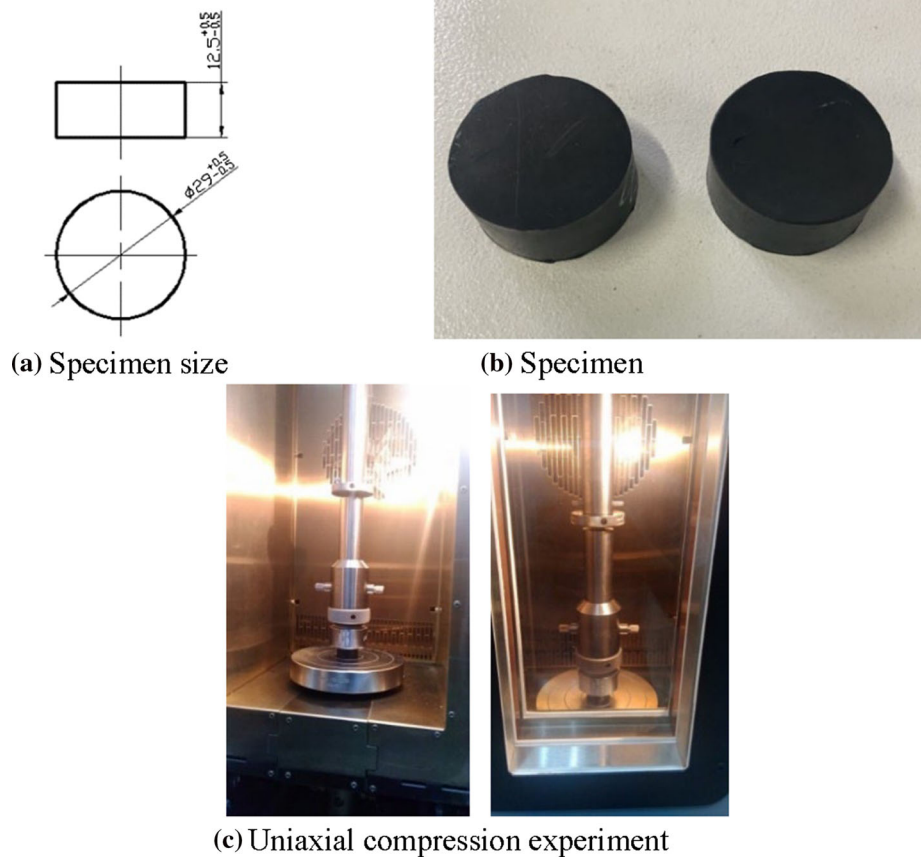
Uniaxial Tension Experiment

According to ISO 37:2011, the specimens were machined into dumbbell-type specimens [24] with a length of 25 ± 0.5 mm and a thickness of 2.0 ± 0.2. Due to the vulcanization errors, the thickness and width of the specimen at different positions were measured for several times, and the average value was obtained. In the experiment, the stretching speed was 500 mm/min. The uniaxial stretching experiment process is shown in Fig. 2.

Uniaxial Compression Experiment

According to ISO 3384:2005, the standard specimen diameter is 29 ± 0.5 mm and height is 12.5 ± 0.5 mm [25]. At the beginning of the experiment, the initial height and diameter of the specimen were measured. During the experiment, the compression speed was 10 mm/min and the compression deformation was 3.75 mm (30% of the specimen height). Then, the specimen was relaxed at the same rate. The process of uniaxial compression experiment is shown in Fig. 3.

Compressive Stress Relaxation Experiment

According to ISO 7743:1989, the specimens were compressed uniaxially as shown in Fig. 3. After thermal and mechanical conditioning of the specimens, they were kept in the holding tank for more than 30 min [26]. The specimens were continued to be compressed at 150 °C. The compression deformation is 3.75 mm and the compression speed is 10 mm/min. The compression state was maintained for 300 s, and then the specimens were relaxed at the same rate.

Experiment Result

The stress–strain data in the axial direction were obtained by uniaxial tension and uniaxial compression experiment experiments. The least squares method was used to fit the stress–strain data. By comparing different models with the original experiment curves, the Yeoh model with higher fitting accuracy was used.

The curve fit of the Yeoh model to the experiment data is shown in Fig. 4, and the correlation coefficient is 0.983, indicating that the accuracy is high. The Yeoh model can
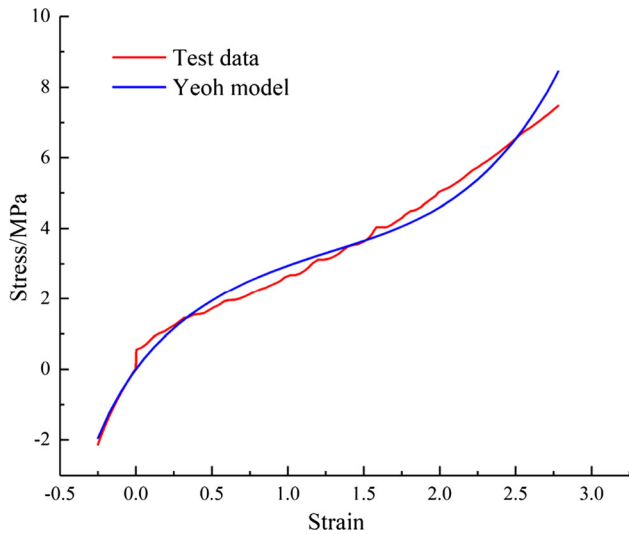
J Fail. Anal. and Preven. (2022) 22:841–857

845

Fig. 4 Yeoh model fitting curve

Table 1 Yeoh model parameters

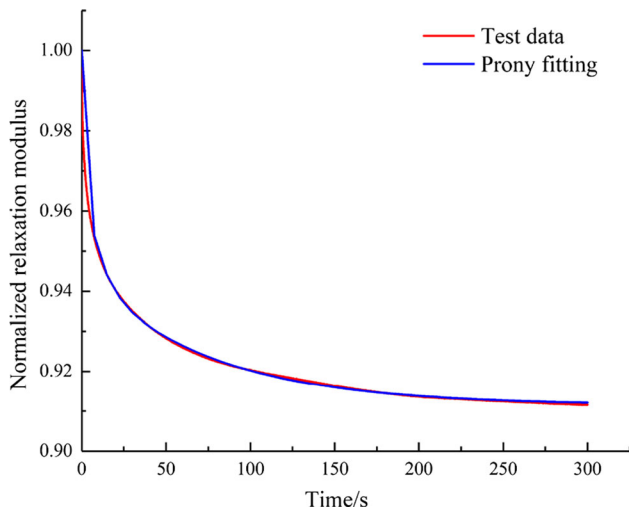| Model	Parameters
Yeoh	$C_{10} = 0.973292$, $C_{20} = -0.039600$, $C_{30} = 0.002626$

Fig. 5 Prony level fitting curve

be used. The parameters of the Yeoh model are shown in Table 1.

Stress time data were obtained by compressive relaxation experiments. After normalizing the stresses, the same least squares method was used for fitting. The fit is shown in Fig. 5, and the correlation coefficient is 0.992, which is a high fitting accuracy. The fitted parameters can be used. The parameters of the Prony level are shown in Table 2.

Table 2 Prony level parameters

$\overline{g}_1^p$	$\overline{\tau}_1^p$	$\overline{g}_2^p$	$\overline{\tau}_2^p$	$\overline{g}_3^p$	$\overline{\tau}_3^p$
0.0312	85.08318	0.02874	0.75362	0.0293	10.88513

Constitutive Model Validation

To verify the correctness of the parameters of the hyperelastic model, an FEA model is established, as shown in Fig. 6. The model dimensions and loading were the same as in the uniaxial tension experiment. The experiment data are engineering stress–engineering strain data, which are transformed into true stress–true strain according to Eqs. 9 and 10. The real stress–real strain at the center of the specimen was extracted and compared with the experiment data, as shown in Fig. 7. Among them, the correlation coefficient is 0.997, which proves that the hyperelastic model parameters are correct.

$$\sigma_T = \sigma_N(1 + \varepsilon_N) \tag{Eq 9}$$

$$\varepsilon_T = \ln(1 + \varepsilon_N) \tag{Eq 10}$$

where σ_T is the true stress, σ_N is the engineering stress, ϵ_T is the true strain, and ϵ_N is the engineering strain.

To verify the correctness of the parameters of the viscoelastic model, an FEA model is established, as shown in Fig. 8. It can simulate uniaxial compression and compression relaxation experiments. The y-directional support reaction force RF2 of the upper platen is extracted and converted into stresses according to Eq. 11. The stress time data comparison between experiment and simulation is shown in Fig. 9. Among them, the correlation coefficient is 0.999, and the experiment value matches well with the simulation. So, the Prony level parameter is correct.

$$\sigma = \frac{4 \times RF_2}{\pi \times d_0^2} \tag{Eq 11}$$

where $d_0 = 29$ mm and RF_2 is the y-directional support reaction force of the upper pressure plate.

FEA Model

Establish FEA Model

A 2D axisymmetric model was established. The FEA model of the packer with standard parameters is shown in Fig. 10(a). The outer diameter and height of the calking ring are 115 mm and 10 mm. The inner and outer diameters of the packing element are 80 mm and 114 mm, and the height of the packing element is 70 mm. The inner diameter of the center pipe is 60 mm, the outer diameter of the casing is 139.7 mm, and the wall thickness is 6.98 mm.

846

J Fail. Anal. and Preven. (2022) 22:841–857

Fig. 6 FEA model of dumbbell-shaped specimen

(a) Geometric model   **(b)** Mesh model

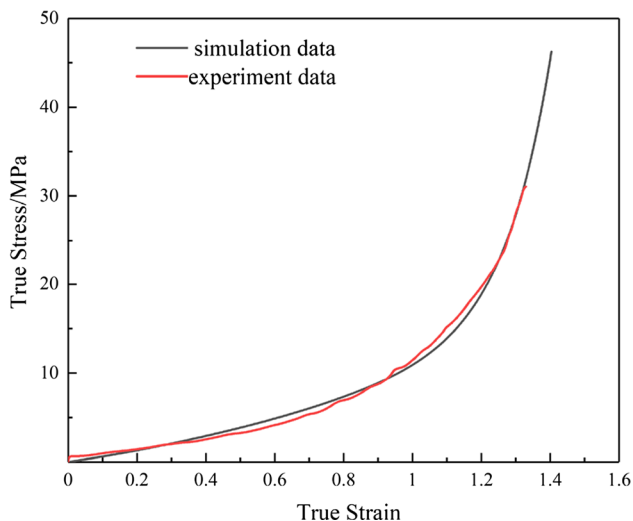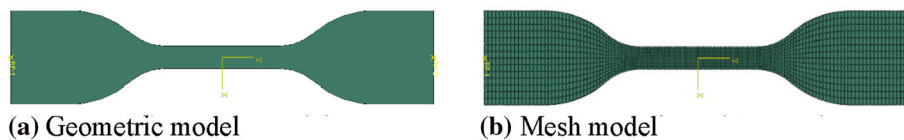**Fig. 7** Comparison of uniaxial tension experiment and simulation

Fig. 9 Comparison of compression experiment and simulation

Fig. 8 FEA model of cylindrical specimen

(a) Geometric model   **(b)** Mesh model

The upper and lower rounding radius of the packing element is R = 2 mm, and the upper and lower calking ring rounding is r = 2 mm.

The packer grid model is shown in Fig. 10(b). The grid of the packing element uses CAX4RH units, and the rest of the component grids use CAX4 units. Among them, the global cloth size on the packing element is 0.5, and there are a total of 5038 units. In addition, the friction coefficient between the packing element and the casing, the center pipe and the spacer ring are defined as 0.3, and the friction coefficient between the spacer ring and the center pipe is defined as 0.1 [27]. Figure 10(c) shows the nodal path of the contact pressure extracted in the text.

Material Properties and Analysis Steps Setting

In the FEA model, the hyperelastic parameters and Prony series parameters of the packing element material need to be set. Then, select instantaneous in the moduli timescale (for viscoelasticity), which means the packing element setting is an instant process, only reflecting the hyperelastic properties. During the pressure-bearing stage, due to the long working time of the packer downhole, the packing element additionally exhibits viscoelasticity.

Two analysis steps were set. The first analysis step was static, general, and the analysis step time is 1s. The second analysis step was viscous (Visco), and the analysis step time is 500s, so that the packing element has enough time for the stress relaxation effect.
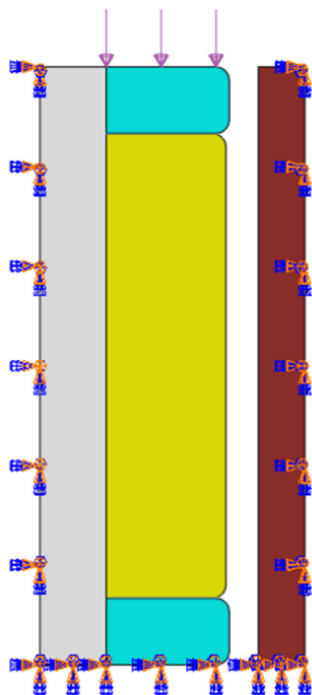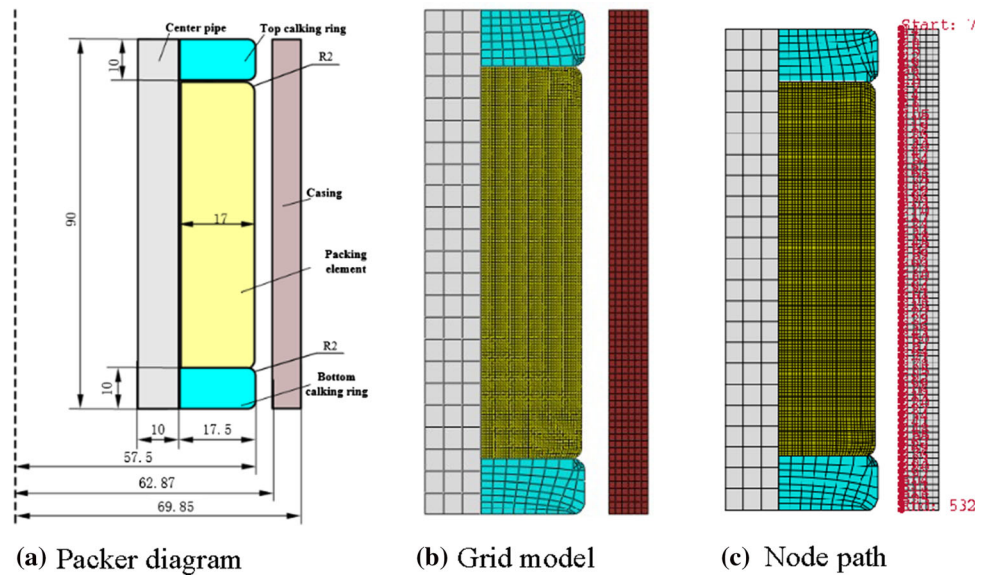
Fig. 10 FEA model of packer

(a) Packer diagram   **(b) Grid model**   **(c) Node path**

Fig. 11 Boundary condition of the FEA model

Fig. 12 Schematic diagram of the visual experiment setup

ring, which is expressed that the position of the upper spacer ring has been fixed, and the position of the packer is locked after entering the viscosity analysis step. Therefore, the conversion of setting method can be avoided, and the simulation time can be saved.

FEA Model Verification

Visualization Experiment

To verify the accuracy of the FEA model, a visualization experiment setup was designed for observing the deformation of the packing element. Using a non-contact full-field strain measurement system, the deformation of the packing element was quantitatively recorded. Finally, the experiment results were compared with the FEA results to verify the accuracy of the FEA model.

The visual experiment setup is shown in Fig. 12. It mainly consists of four parts, which are a packing element sealing simulation system, a measurement system, a hydraulic system, and a loading system.

Boundary Condition Setting

Figure 11 shows the boundary conditions of the FEA model of the packer, in which the casing, the center pipe, and the lower spacer ring are completely fixed, and a setting load is applied to the surface of the upper spacer ring. To simulate the locking action of the packing element after setting, in the Visco analysis step, a specific boundary condition (fixed at current position) should be set for the upper spacer
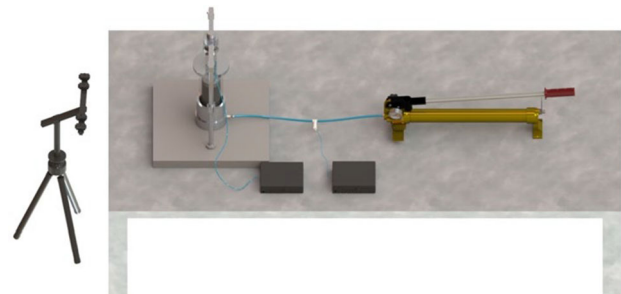
848

J Fail. Anal. and Preven. (2022) 22:841–857

Fig. 13 The actual packager visualization experiment bench
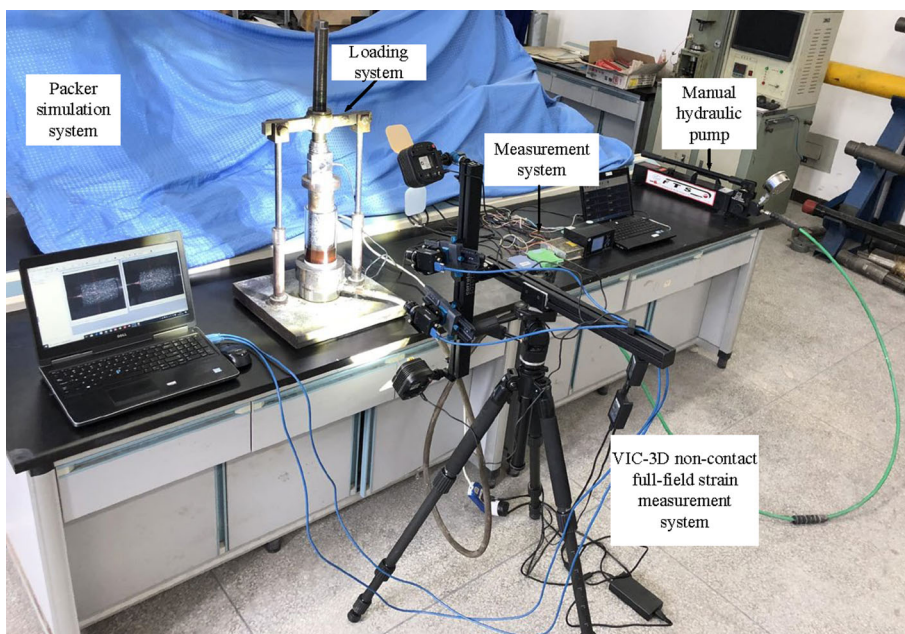
Table 3 Packer visualization experiment scheme

Experiment number	Rubber hardness/SHA	Packer height/mm	Axial load/N
1	80	70	2000
2			2100
3			2200

Table 4 Experiment results

Experiment number	Axial strain	Tangential strain
1	− 0.1653	0.2389
2	− 0.1589	0.2669
3	− 0.1527	0.3031

The visual experiment device physical diagram is shown in Fig. 13. Under the action of a thrust ball bearing, the effect of torque is eliminated, and only axial pressure load is transmitted downward. The rotating lead screw transmits the axial load downward, and the gravity sensor is used to control the magnitude of the axial load loaded in the experiment, i.e., the seating load of the sealer cartridge. What's more, the VIC-3D non-contact full-field strain measurement system is used to quantitatively observe. Finally, the deformation of the packing element was recorded.

Experiment Program and Results

To study the deformation of the packing element during work, 80SHA HNBR material was selected for the visualization experiment. The height of the packing element was 70 mm. Three experiments with different axial loads were carried out. The specific experiment program is shown in Table 3.

After the experimental setup was installed, turned on all experimental units. The liquid was pumped into the annulus with a manual hydraulic pump, and the pressure was stabilized for 10 minutes to ensure no leakage. It should be noted that it is necessary to rotate the lead screw to reciprocate five times to eliminate the rubber hysteresis effect. The VIC-3D non-contact full-field strain measurement system was debugged to work normally. After loading by rotating the lead screw, the maximum axial strain and maximum tangential strain of packing elements were recorded from the measurement system. The experiment results are shown in Table 4.

FEA Simulation and Results Comparison

According to the structural dimensions of the experiment device, a 2D axisymmetric FEA model was established, as shown in Fig. 14. Loading settings were consistent with the experiment. The maximum axial strain and the maximum tangential strain of the packing element were extracted and compared with the experiment results. The specific data are shown in Table 5.

By comparing with the experiment data, the error is within 10%, as shown in Fig. 15. This is because the rubber material was vulcanized, resulting in non-uniform dispersion of carbon black, filler, etc., resulting in the rubber being anisotropic, while the FEA simulation assumes the rubber material to be isotropic. This error range is allowed in engineering. So, the FEA model is accurate.

The Influence of Stress Relaxation on the Packer Performance

Under standard size parameters, taking a setting load of 30 MPa as an example, the effect of stress relaxation behavior on the sealing performance of the packer is analyzed.

When the packer has just been set, the peak shear stress is 46.54 MPa, which appears at the shoulder of the packing element, as shown in Fig. 16(a). This is because the continuous pressure makes the packing element material squeeze into the annulus between the spacer ring and the casing. The shoulder area has the largest shear deformation comparing with other parts. As the spacer ring
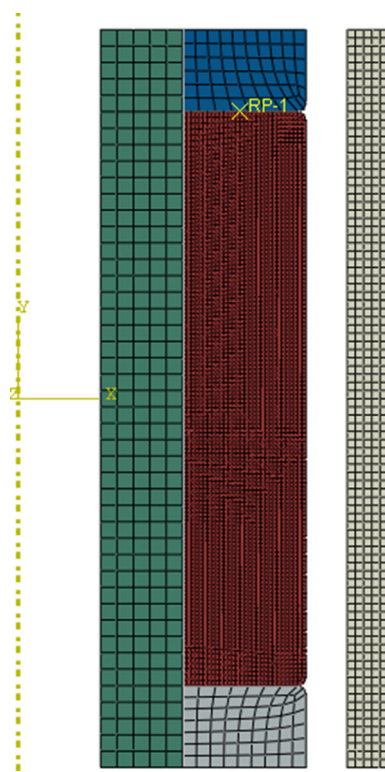

Fig. 14 Packer visualization setup FEA model

continuously compresses the packing element, the probability of cutting damage will increase. At 150 °C, the packing element is compressed for a long time, and the rubber material exhibits stress relaxation. The peak shear stress is reduced to 43.3 MPa, a decrease of 6.9%, but the distribution of shear stress is almost unchanged, as shown in Fig. 16(b).

Von Mises stress is another indicator for evaluating rubber failure. To judge the strength of the packer, the stress values before and after stress relaxation were calculated, as shown in Fig. 17. Before the stress relaxation, it can be seen from Fig. 17(a) that the peak von Mises stress value is 22.72 MPa, which appears on the shoulder, being the contact position of the chamfer of the spacer ring and the packing element. Because the spacer ring continuously compresses the packing element, the appearance of the packing element is greatly changed at the shoulder, causing local stress concentration, and the peak von Mises stress value appears, which increases the chance of failure of the packing element. After the stress relaxation, the peak von Mises stress value is reduced to 20.37 MPa, a decrease of 10.3%, and the stress distribution is almost unchanged, as shown in Fig. 17(b).

Figures 18 and 19 show the distribution of contact stress before and after stress relaxation. It can be seen from Fig. 18(a) that the peak contact stress is 21.22 MPa. When the packing element undergoes stress relaxation, the peak contact stress is decreased to 19.79 MPa, which is a 6.7% reduction. The contact stress distribution is almost unchanged, as shown in Fig. 18(b). In the meantime, it can be found from Fig. 19 that the peak contact stress appears at about 30 mm of the node path on the casing. The overall contact stress is distributed in a "saddle-like" shape. Before and after the stress relaxation, the contact length does not change much, but the stress value drops significantly. The contact stress on the contact length of the packing element and the casing is reduced, which leads to the weakening of the packer sealing performance.

Before and after stress relaxation, Table 6 shows the changes in peak shear stress, peak von Mises stress, and peak contact stress. It can be found that the peak shear

Table 5 Experiment result and FEA result

Experiment number	Experiment result		FEA result		Relative error	
	Axial strain	Tangential strain	Axial strain	Tangential strain	Axial strain /%	Tangential strain /%
1	− 0.1527	0.2389	− 0.1571	0.2399	2.881	0.419
2	− 0.1589	0.2669	− 0.1640	0.2834	3.210	6.182
3	− 0.1653	0.3031	− 0.1675	0.2950	1.331	2.672

850

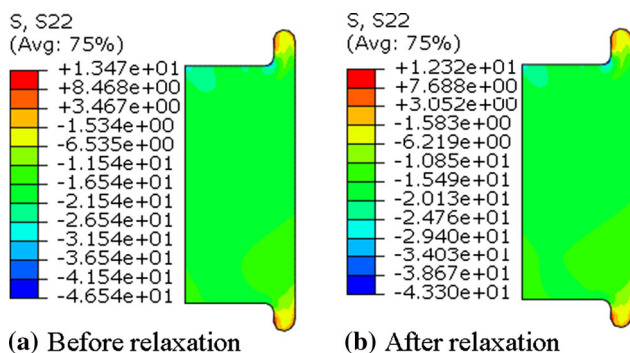J Fail. Anal. and Preven. (2022) 22:841–857
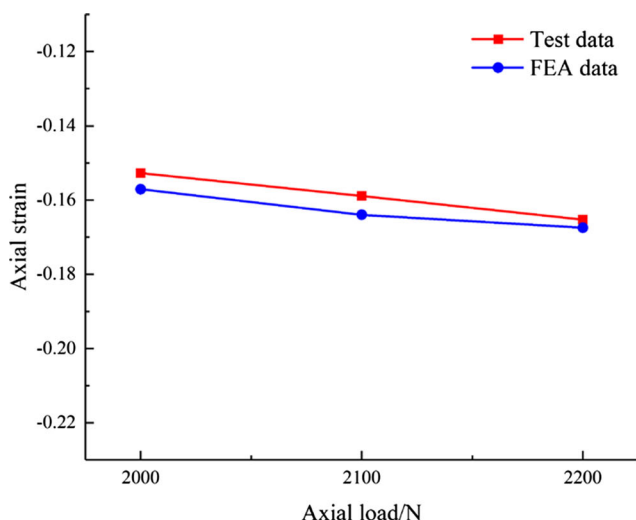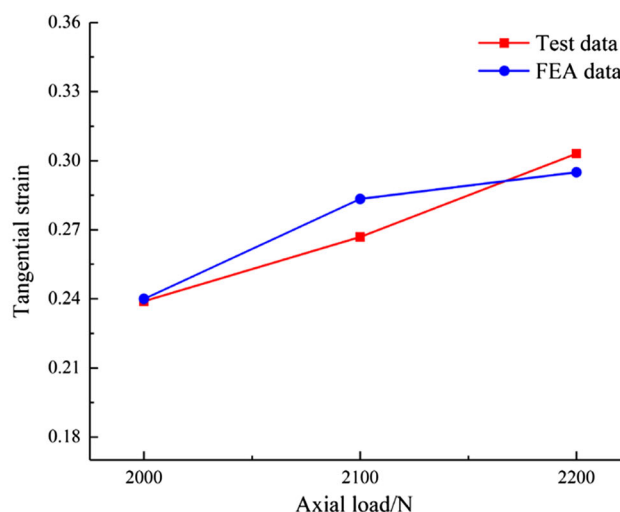
(a) Axial strain

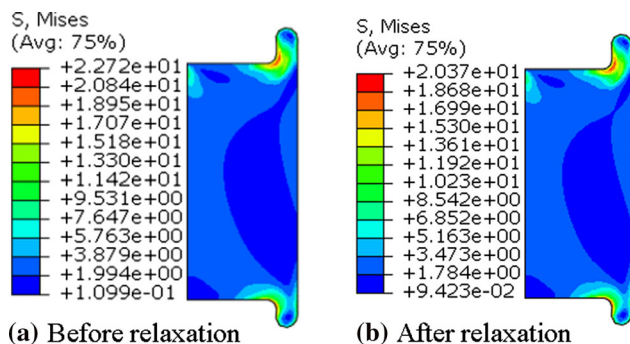**(b)** Tangential strain

Fig. 15 Comparison of experiment results and FEA results

(a) Before relaxation   **(b)** After relaxation

Fig. 16 The distribution of shear stress before and after relaxation

(a) Before relaxation   **(b)** After relaxation

Fig. 17 Von Mises stress distribution

stress has dropped by 6.9%, the peak Mises stress has dropped by 10.3%, and the peak contact stress has dropped by 6.7%. This is because the rubber will quickly deform now of external force. The viscous effect makes the internal stress of the rubber in an unbalanced state. As time goes on, the macromolecules curled and entangled in the

rubber slowly deform under the stress; then a relative displacement occurs between the macromolecules, resulting in a constant total deformation of the rubber. Under the circumstances, the stress decays continuously [28]. It can be concluded that although the stress relaxation phenomenon will play a certain protective effect on the packing element, the reduction in the peak contact stress on the sealing interface should be considered in engineering; otherwise, it will cause sealing failure, causing a safety accident eventually.

The Influence of Key Parameters on the Packer Sealing Performance

Since stress relaxation has a certain influence on the sealing performance of the packer at 150 °C, this section analyzes the influence of various key parameters on the sealing performance of a packing element under stress relaxation.

The Influence of Setting Load on Packer Performance

When the packer is run downhole, a certain setting load is required to ensure its proper operation. Too small setting loads can easily cause the packer to fail to meet the sealing requirements, and too large setting loads can lead to poor performance of the packer. Therefore, in this section, the influence of different setting loads on the performance of the packing element is analyzed. The size of the packer is a standard parameter.

Contact stress distribution curves on the casing under different setting loads are shown in Fig. 20. The contact

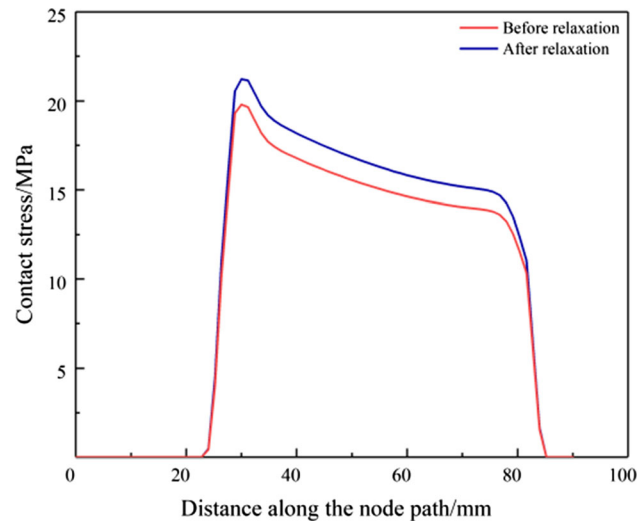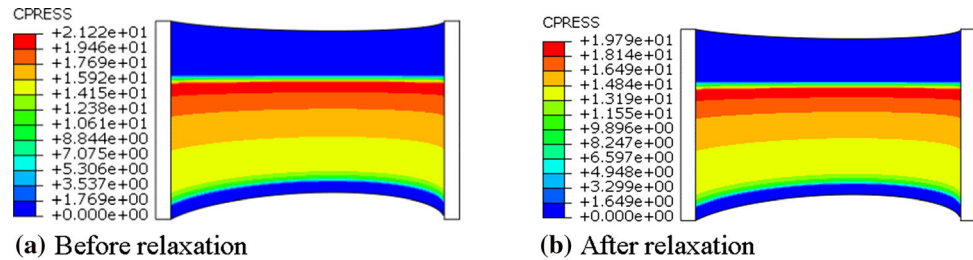**Fig. 18** The distribution of contact stress on the casing

(a) Before relaxation

(b) After relaxation

Fig. 19 Contact stress curve along the node path

Fig. 20 Distribution of contact stress under different setting loads

Table 6 Changes in the mechanical properties of the packing element

	Peak shearing stress	Peak Mises stress	Peak contact stress
Before relaxation/MPa	46.54	22.72	21.22
After relaxation/MPa	43.30	20.37	19.79
Rate of stress change/(%)	6.9	10.3	6.7

stress on the casing is unevenly distributed along the length of the casing. With the increase in setting load, the unevenly distributed degree becomes higher. This is because: in the process of loading and compression, the packing element has radially deformed, and the outer surface of the middle part of the packing element first contacts the inner wall of the casing. Currently, there is friction between the packing element and the casing. As the packing element continues to compress, part of the work done by the axial force will be consumed by friction, thus weakening the force at the lower part of the compression packing element, leading to uneven radial deformation of the packing element, and thus resulting in uneven distribution of contact stress on the casing. Furthermore, when
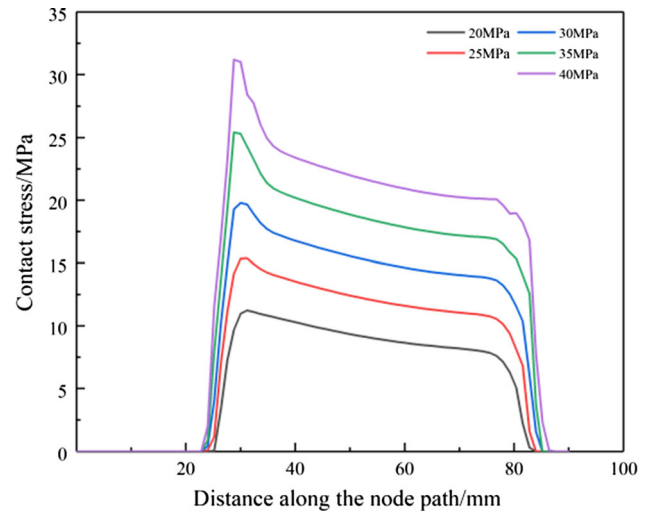
the setting load increases, the area of contact increases, and the friction work to be overcome also increases, which makes the radial deformation of the packing element more uneven. The contact stress distribution also becomes more uneven. At the same time, with the increase in setting load, the peak contact stress gradually increases, and the effective sealing length increasingly becomes longer, which is conducive to improving the sealing performance of the packing element.

Before and after stress relaxation, the variation patterns of peak shear stress, peak von Mises stress, and peak contact stress are shown in Fig. 21. As can be seen from Fig. 21(a) and (c), with the increase in setting load, the peak shear stress and peak contact stress increase continuously, and the change amount of stress before and after stress relaxation increases consequently. It can be seen from Fig. 21(b) that the peak von Mises stress increases with the increasing of setting load, but the change of von Mises stress increases first and then decreases before and after stress relaxation.

Before and after stress relaxation, the specific changes of mechanical properties under different setting loads are shown in Table 7. Increasing the setting load is a powerful means to improve the sealing performance. However, due to space limitation of the packing element, the excessive
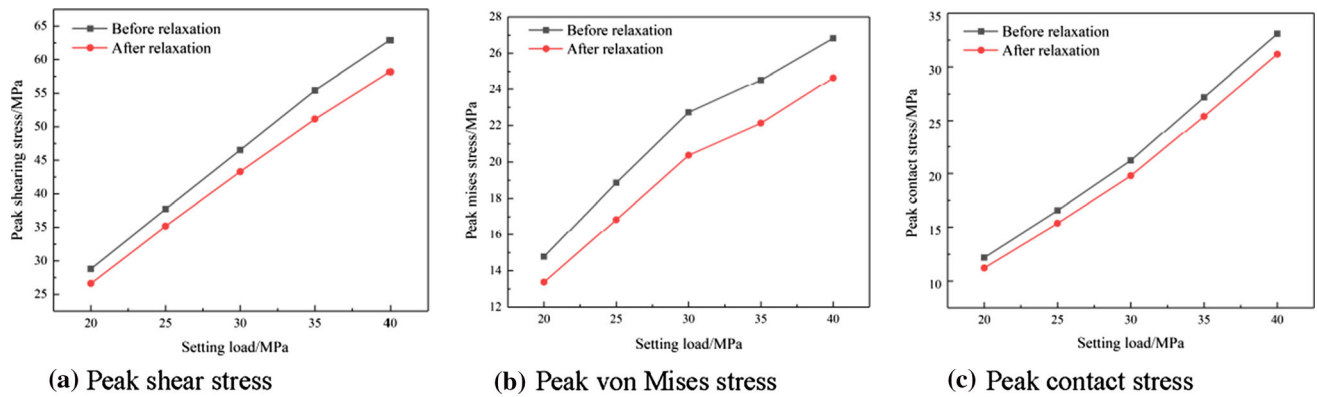
852

J Fail. Anal. and Preven. (2022) 22:841–857

(a) Peak shear stress (b) Peak von Mises stress (c) Peak contact stress

Fig. 21 The changes of mechanical properties under different setting loads

Table 7 Mechanical properties under different setting loads

Setting load/ MPa	Peak shearing stress/MPa			Peak von Mises stress/MPa			Peak contact stress/MPa		
	Before relaxation	After relaxation	Stress change	Before relaxation	After relaxation	Stress change	Before relaxation	After relaxation	Stress change
20	28.82	26.63	2.19	14.77	13.37	1.40	12.19	11.22	0.97
25	37.72	35.17	2.55	18.87	16.84	2.03	16.56	15.37	1.19
30	46.54	43.3	3.24	22.72	20.37	2.35	21.22	19.79	1.43
35	55.41	51.15	4.26	24.53	22.13	2.40	27.19	25.41	1.74
40	62.88	58.17	4.71	26.83	24.65	2.18	33.09	31.19	1.90

von Mises stress will occur, which will lead to crushing failure of the packer. Therefore, for safety sealing reasons, it is recommended that the setting load range is 30–35MPa, and the strength of the packing element should be increased, such as using fluorine rubber with medium–high hardness and high temperature resistance as the packing element material or using the packing element with anti-shoulder rib plate.

The Influence of the Height on the Packer Performance

When the height of the packing element is too high, it will cause unstable deformation, resulting in uneven force and greater damage to the packing element [29]. Selecting a suitable height of the packing element can not only avoid the unstable deformation, but also reduces the waste of materials. Therefore, in this section, under a setting load of 30 MPa, a certain range of the heights were selected, and the influence of different height of the packing element was analyzed.

The contact stress distribution at different heights is shown in Fig. 22. With the continuous increase in the height, the peak contact stress has a slight change, firstly decreasing and then increasing, and the minimum is 21.22 MPa at the height of 70 mm. The increase in the height enhances the contact length, which is beneficial to
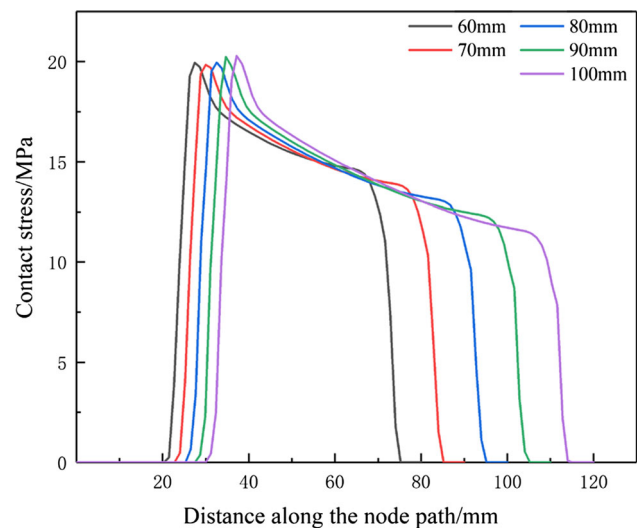
Fig. 22 The contact stress distribution at different heights

improve the sealing performance of the packer. In the meantime, raising the height results in a more uneven distribution of contact stress among the length. The reason is that the longer the packing element, the larger the contact area during constrained deformation, and the greater the impact of friction, and the less conducive to the uniform radial deformation of the packing element. Moreover, with
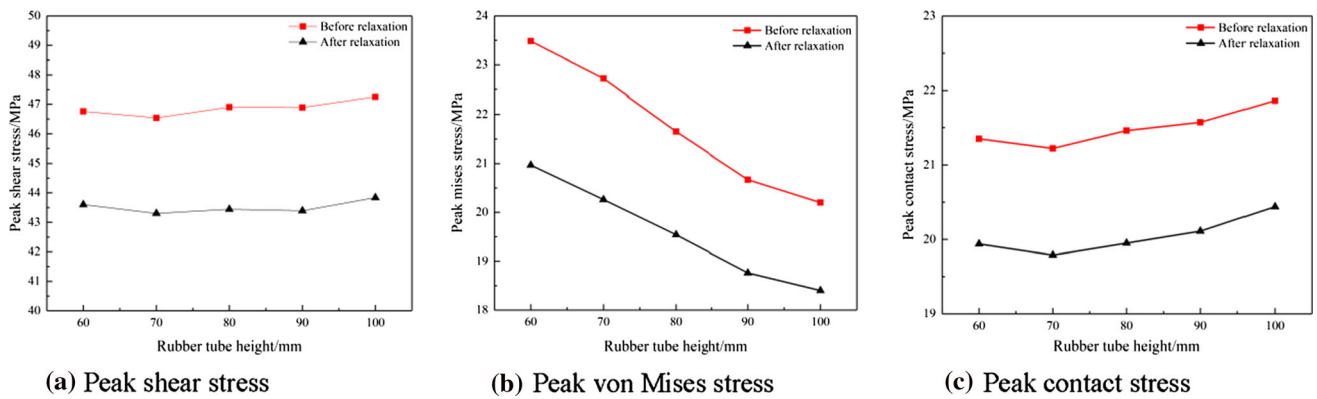
(a) Peak shear stress   **(b) Peak von Mises stress**   **(c) Peak contact stress**

Fig. 23 Changes in the mechanical properties under different heights

Table 8 Mechanical properties at different heights

Packing element height/mm	Peak shearing stress/MPa			Peak von Mises stress/MPa			Peak contact stress/MPa		
	Before relaxation	After relaxation	Stress change	Before relaxation	After relaxation	Stress change	Before relaxation	After relaxation	Stress change
60	46.76	43.60	3.16	23.48	20.97	2.51	21.35	19.94	1.41
70	46.54	43.30	3.24	22.72	20.26	2.46	21.22	19.79	1.43
80	46.90	43.44	3.46	21.65	19.54	2.11	21.46	19.95	1.51
90	46.89	43.39	3.50	20.67	18.76	1.91	21.57	20.11	1.46
100	47.25	43.84	3.41	20.20	18.40	1.80	21.86	20.44	1.42

the increase in the height, the position of the peak contact stress gradually moves away from the loading end.

Before and after stress relaxation, the changes in the mechanical properties at different heights are shown in Fig. 23. It can be seen from Fig. 23(a) that the height has little effect on the peak shear stress and has little effect on the change of the peak shear stress. It can be drawn from Fig. 23(b) that the increase in the height will significantly reduce the peak von Mises stress, which better improves the stress concentration on the packing element and reduces the risk of failure. In addition, the amount of the peak von Mises stress change decreases accordingly. As shown in Fig. 23(c), when the height increases, the peak contact stress first decreases and then increases, which has little effect on the change regarding stress relaxation.

Before and after stress relaxation, Table 8 shows the specific changes of the mechanical properties at different heights. It can be clearly seen that the increase in the height has little effect on the peak shear stress and peak contact stress, but it can significantly reduce the peak von Mises stress, which has a certain protective effect on the packing element. The packing element is better not to be too high, to avoid deformation and instability, which will affect the sealing performance.

The Influence of the Inner Diameter on the Packer Performance

The inner surface of the packing element is close to the outer wall of the center pipe. When the inner diameter of the center pipe is determined, changing the inner diameter will not only affect the wall thickness of the center pipe, but also affect the thickness of the packing element. If the inner diameter of the packing element is too small, it will weaken the strength of the center pipe. If its inner diameter is too large, the packing element will be too thin, so it is difficult to ensure the seal. Therefore, in this section, under the setting load of 30 MPa, the influence of different inner diameters on the performance of the packer is analyzed.

The contact stress distribution on the casing under different inner diameters is shown in Fig. 24. With the continuous increase in the inner diameter, the location of the peak contact stress is continuously farther away from the loading end, and the contact length is continuously reduced, which is unbeneficial to sealing. This is because the increase in the inner diameter lessens the volume of the packing element, and the rubber is approximately incompressible. To fill the gap between the packing element and the casing, the axial compression distance will continue to

854

J Fail. Anal. and Preven. (2022) 22:841–857

increase. In addition, it can be found that the peak contact stress is the largest at the inner diameter of 74 mm.

Before and after stress relaxation, the changes in the mechanical properties at different inner diameters are
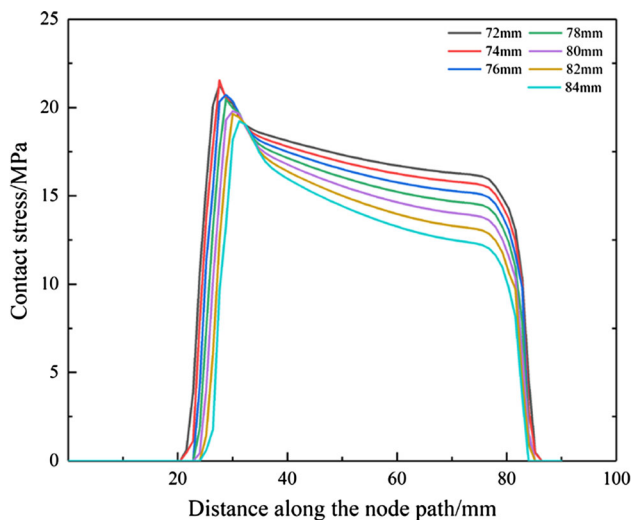

Fig. 24 The contact stress distribution under different inner diameters

shown in Fig. 25. It can be seen from Fig. 25(a) that as the inner diameter increases, the peak shear stress first increases and then decreases. Among them, when the inner diameter is 76 mm, the peak shear stress is the largest. After relaxation, its value is 45.37 MPa, and the risk of shear failure is the greatest. It can be seen from Fig. 25(b) that as the inner diameter increases, the peak von Mises stress continues to decrease, which weakens the stress concentration phenomenon and reduces the probability of failure. It can be obtained from Fig. 25(c) that when the inner diameter increases, the peak contact stress first increases and then decreases. When the inner diameter is 74 mm, the peak contact stress is the largest. Further speaking, the sealing performance is the best. Table 9 shows the specific changes in the mechanical properties at different inner diameters.

The Influence of the Outer Diameter on the Packer Performance

The gap between the packing element and the casing is one of the key factors affecting the performance. The smaller the gap, the more difficult it is to run the packer. The larger the gap, the worse the sealing performance of the packer
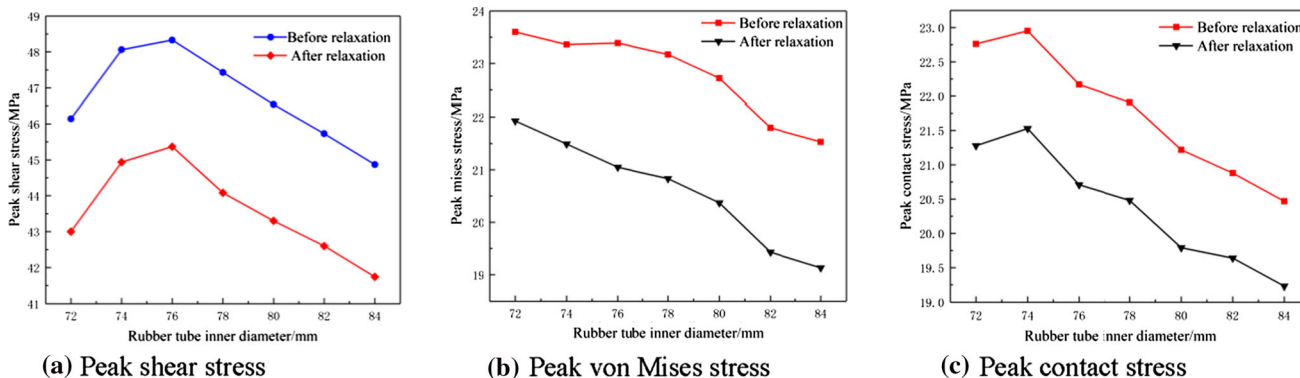

(a) Peak shear stress   **(b)** Peak von Mises stress   **(c)** Peak contact stress

Fig. 25 Changes in mechanical properties under different inner diameters

Table 9 Mechanical properties under different inner diameters

Packing element inner diameter/mm	Peak shearing stress/MPa			Peak von Mises stress/MPa			Peak contact stress/MPa		
	Before relaxation	After relaxation	Stress change	Before relaxation	After relaxation	Stress change	Before relaxation	After relaxation	Stress change
72	46.14	43.00	3.14	23.60	21.93	1.67	22.76	21.28	1.48
74	48.06	44.94	3.12	23.36	21.49	1.87	22.95	21.53	1.42
76	48.33	45.37	2.96	23.39	21.05	2.34	22.17	20.71	1.46
78	47.43	44.08	3.35	23.17	20.83	2.34	21.91	20.48	1.43
80	46.51	43.30	3.21	22.72	20.37	2.34	21.22	19.79	1.43
82	45.73	42.60	3.13	21.80	19.43	2.37	20.88	19.64	1.64
84	44.87	41.74	3.13	21.53	19.13	2.4	20.47	19.23	1.24

[30]. When the casing type is determined, changing the outer diameter of the packing element will change the gap and the volume of the packing element. Therefore, this section analyzes the influence of the outer diameter on the packer sealing performance when the setting load is 30 MPa.

Figure 26 shows the contact stress distribution with different outer diameters. When the outer diameter increases, the peak contact stress continues to increase, and the contact length continues to increase, and the contact stress is more evenly distributed along the length. This is because the increase in the outer diameter causes the gap to decrease continuously, the axial compression distance decreases, and the overall radial deformation is more fully and uniform. Under the premise of ensuring that the packer goes down the well, the outer diameter should be increased as much as possible to improve the sealing performance of the packer. At the same time, as the outer diameter increases, the peak contact pressure is closer to the loading end. Compared with the change of the inner diameter, the

change in the peak contact stress position caused by the change of the outer diameter is larger. This is because under the same change amount, changing the outer diameter has a greater change in the volume of the packing element, thus making the change in the circumferential compression distance greater.

Before and after stress relaxation, the changes in the mechanical properties under different outer diameters are shown in Fig. 27. It can be seen from Fig. 27(a) that as the outer diameter increases, the peak shear stress before and after stress relaxation similarly decreases linearly, and the amount of shear stress change before and after stress relaxation becomes smaller and smaller. As Fig. 27(b) shows, when the outer diameter increases, the peak von Mises stress element decreases like a parabola, and the influence of the stress relaxation on the peak von Mises stress is gradually weakened. Figure 27(c) shows that as the outer diameter continues to increase, the peak contact stress gradually decreases. When the outer diameter is 122 mm, the change in peak contact stress is the smallest, which is 0.87 MPa. The specific changes in the mechanical properties before and after stress relaxation under different outer diameters are shown in Table 10.

In summary, it can be clearly seen from Fig. 27 that increasing the outer diameter can better reduce the peak shear stress and peak von Mises stress, reduce the risk of shear damage, and extend the packer service life. Increasing the outer diameter can effectively improve the sealing performance of the packer and ensure the stable operation of the packer. According to the design requirements of the packer, the gap between the packing element and the casing should be in the range of 3 to 5 mm to ensure that the packer can successfully reach the well [1]. Therefore, the optimal height of the packing element studied is 122mm. It can be concluded that under the premise of ensuring that the packer goes down the well, increasing the outer diameter is one of the effective measures to improve the sealing performance.
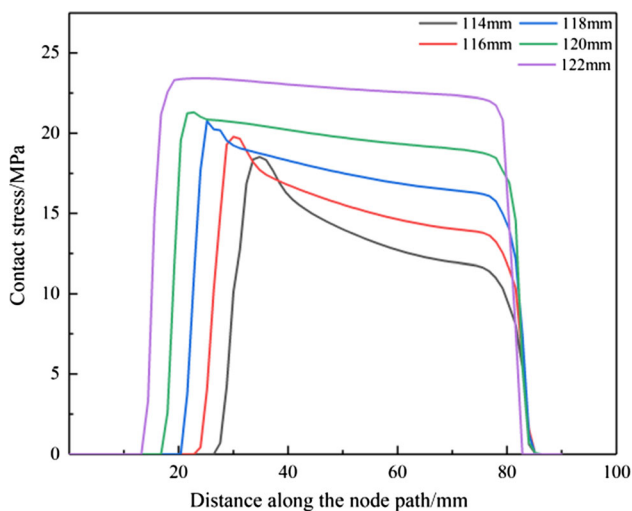

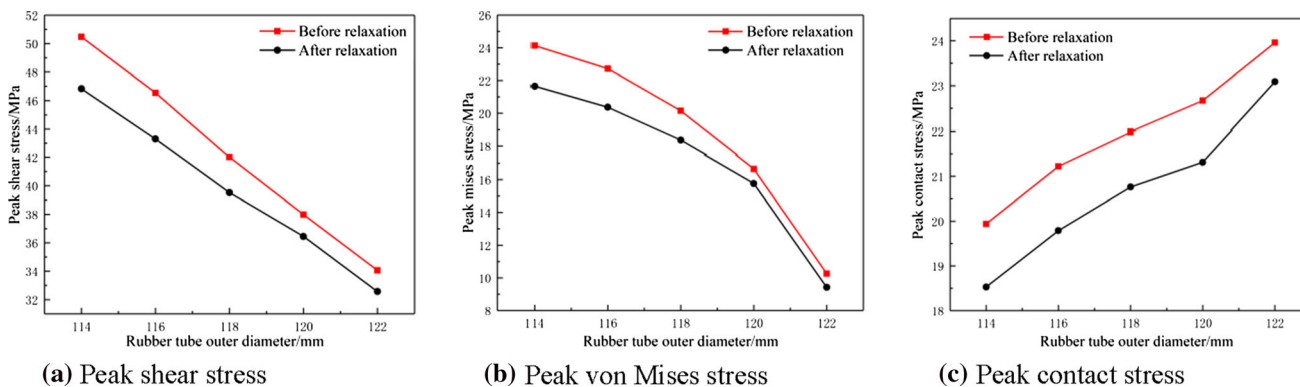Fig. 26 The contact stress distribution with different outer diameters

(a) Peak shear stress

(b) Peak von Mises stress

(c) Peak contact stress

Fig. 27 Changes in mechanical properties under different outer diameters

856

J Fail. Anal. and Preven. (2022) 22:841–857

Table 10 Mechanical properties under different outer diameters

Packing element outer diameter/mm	Peak shearing stress/MPa			Peak von Mises stress/MPa			Peak contact stress/MPa		
	Before relaxation	After relaxation	Stress change	Before relaxation	After relaxation	Stress change	Before relaxation	After relaxation	Stress change
114	50.47	46.83	3.64	24.13	21.65	2.48	19.94	18.53	1.41
116	46.54	43.30	3.24	22.72	20.26	2.46	21.22	19.79	1.43
118	42.01	39.53	2.48	20.16	18.36	1.80	21.98	20.76	1.22
120	37.98	36.45	1.53	16.65	15.76	0.89	22.67	21.34	1.33
122	34.06	32.57	1.49	10.26	9.42	0.84	23.96	23.09	0.87

Conclusion

In this paper, aiming at the problem of sealing failure and rupture of packing elements under HTHP, the rubber uni-axial tension, uniaxial compression, and compression relaxation tests were carried out and the 2D FEA model of packing element was established. The sealing performance and strength behavior of the packer under HTHP before and after stress relaxation were analyzed. At the same time, the sensitivity analysis of key parameters was carried out and the following conclusions were obtained.

(1) Due to the stress relaxation phenomenon of the rubber, the peak shear stress and peak von Mises stress on the packing element are reduced, which reduces the risk of the packing element being torn and damaged and prolongs the service life of the packing element. At the same time, the stress relaxation will also reduce the peak contact stress, resulting in a decrease in the sealing performance. Therefore, the influence of the stress relaxation must be considered in the process of evaluating sealing performance.

(2) Increasing the setting load is a powerful means to improve the sealing performance, and the main reason to lead to the crushing failure of packers. It is recommended that the setting load range is 30–35MPa, and the strength of the packing element should be increased.

(3) When the height of the packing element is increased, the peak shear stress and peak contact stress do not change much, but the peak von Mises stress can be significantly reduced, which has a certain protective effect on the packing element. However, the packing element is better not to be too high, to avoid deformation and instability, which will profit the sealing performance.

(4) With the increase in the inner diameter, the peak shear stress and peak contact stress show a trend of first increasing and then decreasing within the range of dimensions studied, and the peak von Mises stress decreases. Considering the strength and sealing performance, the inner diameter of the packing element should not be too large to ensure its thickness, to resist the risk of damage to the packing element.

(5) The increase in the outer diameter of the packing element can better improve its force, increase the contact stress, and make the contact stress distribution more uniform. It not only reduces the risk of damage, but also improves the sealing performance. Due to the limitation of the gap between the packing element and the casing, the optimal height of the packing element studied is 122mm. Therefore, under the condition of ensuring that the packer goes down the well, it is recommended to increase the outer diameter to improve the sealing performance.

Conflict of interest The author of this paper and the co-authors do not have any related financial or non-financial competing interests.

References

1. X.-R. Zhu, *The basics of packer design*. (China Petrochemical Press, Beijing, 2012) (in Chinese)
2. A. Zhong, *Challenges for high pressure high temperature applications of rubber materials in the oil and gas industry* (Cham, Springer International Publishing, 2016), p. 65–79
3. W. Yefei, Z. Wei, X. Cuiping, M. Haisen, G. Shasha, Y. Qing, Z. Fulin, Study on components and formulation of liquid gel packer in air drilling. Petrol. Sci. Technol. **29**, 837–849 (2011)
4. Q. Hua, Y.-B. Qin, Analysis of common causes of seal failure of HTHP completion packer. Petrochem. Technol. **25**, 202 (2018). (in Chinese)
5. Z. Liu, S. Li, L. Zhang, F. Wang, P. Wang, L. Han, Y. Ma, H. Zhang, Analysis of sealing mechanical properties of fracturing packer under complex conditions. J. Fail. Anal. Preven. **19**, 1569–1582 (2019)

6. H. Patel, S. Salehi, R. Ahmed et al., Review of elastomer seal assemblies in oil & gas wells: performance evaluation, failure mechanisms, and gaps in industry standards. J. Petrol. Sci. Eng. **179**, 1046–1062 (2019)

7. F. Guo, T.-Z. Wen, Y.-J. Huang, W. Song, X.-H. Jia, Y.-M. Wang, Experiment study on HTHP sealing performance of packer rubber. Lubr. Eng. **45**, 23–27 (2020). (in Chinese)

8. J. Doane, G. Deng, S. Collins, Permanent Production Packer Pushes Limits of Ultra-HPHT Wells. Drilling Contractor. **69**(3), 168–172 (2013).

9. Z. Tong, Q. Ye, J. Qian, Z. Hao, L. Wang, Down-hole Isolation towards High temperature Reservoir Using Packing Elements with Swellable Thermo-plastic Vulcanizates. J. Petrol Sci. Eng. **172**, 964–975 (2019)

10. W. Lan, H. Wang, X. Zhang, S. Chen, Sealing properties and structure optimization of packer rubber under high pressure and high temperature. Petrol. Sci. **16**(3), 632–644 (2019)

11. F.-H. Duan, Z. Li, C.-X. Hou, C.-H. Guo, F.-P. Li, Y.-S. Duan, Study on the properties of HTHP packer cartridge. Oil Field Equipment. **49**, 66–70 (2020). (**in Chinese**)

12. L.-L. Dong, K. Li, B. Li, X.-H. Zhu, M. Xie, Y.-C. Zhang, J. Wang, Study in deep shale gas well to prevent shoulder protruding packer with high pressure sealing. Eng. Fail. Anal. **118**, 104871 (2020)

13. C.-J. Han, X.-F. Peng, L.-T. Li, anchoring mechanical behavior of packer slips and its HTHP experiment analysis. Nat. Gas. Ind. **40**, 76–82 (2020). (in Chinese)

14. C. Zheng, X. Zheng, J. Qin et al., Nonlinear FEA analysis on the sealing performance of rubber packer for hydraulic fracturing. J. Natural Gas Sci. Eng. **85**, 103711 (2021)

15. A.N. Gent, Relaxation Processes in Vulcanized Rubber. II. Secondary relaxation due to network breakdown. J. Appl. Poly. Sci., **6**, 442–448 (1962)

16. B.S.A.W. Webber, Stress relaxation of elastomer compounds. Sealing Technol. **2011**(2), 9–12 (2011)

17. X.-C. Li, C.Q. Li, Study on high temperature mechanical properties of hydrogenated nitrile rubber. Rubber Industry. **67**(09), 652–659 (2020). (in Chinese)

18. L.-N. Wang, H.-C. Sun, W. Sun, L. Qi, L.-C. Sun, D.-H. Meng, Performance Analysis of Globe- Cone Sealing Considering Stress Relaxation Effect. J. Harbin. Instit. Technol. **52**, 156–162 (2020) (in Chinese)

19. W. Wang, S.-G. Zhao, FEA analysis of rubber O-ring seal with stress relaxation. Lubr. Eng. **33**(10), 24–26 (2008). (in Chinese)

20. X.-D. Zhang, X. Yu, Y. Zhang, L. Yang, R.-J. Hao, Stress relaxation analysis of sealing ring based abaqus. Lubr. Eng. **45**(1), 124–128 (2020). (in Chinese)

21. O.H. Yeoh, Some forms of the strain energy function for rubber. Rubber Chem. Technol. **66**(5), 754–771 (1993)

22. O.H. Yeoh, Characterization of Elastic Properties of Carbon-Black-Filled Rubber Vulcanizates. Rubber Chem. Technol. **63**(5), 792–805 (1990)

23. H. Sun, W. Chen, R. Xiao, An equivalence between generalized Maxwell model and fractional Zener model. Mech. Mater. **100**, 148–153 (2016)

24. International Organization for Standardization, 2011. ISO 37: Rubber, vulcanized or thermoplastic- Determination of tensile stress-strain properties. S. International Organization for Standardization, Switzerland.

25. International Organization for Standardization, 2005. ISO 3384: Rubber, vulcanized or thermoplastic- Determination of stress relaxation in compression at ambient and at elevated temperatures. S. International Organization for Standardization, Switzerland.

26. International Organization for Standardization, 1989. ISO 7743: Rubber, vulcanized or thermoplastic-Determination of compression stress-strain properties. S. International Organization for Standardization, Switzerland.

27. Z. Guo, Q. Li, Y. Wang, B. Sun, S. Zhang, Analysis and structural improvement of the rubber part in packer in a way of nonlinearity FEA, International Conference on Mechanic Automation and Control Engineering (MACE 2011). Inner Mongolia, China, pp. 73-76 (2011).

28. M. Zhu, *Rubber chemistry and physics*. (Chemical Industry Press, Beijing, 1996) (in Chinese)

29. F.-Y. Zhang, Y.-F. Zhang, T.-T. Li, H.-C. Shui, C.-C. Dong, J.-M. Yang, Stability analysis of deformation process of packer rubber. Lubr. Eng. **44**(05), 34–39 (2019). (in Chinese)

30. L. Dong, K. Li, X. Zhu, Z. Li, D. Zhang, Y. Pan, X. Chen, Study on high temperature sealing behavior of packer rubber tube based on thermal aging experiments. Eng. Fail Anal. **108**, 104321 (2020)